

# The Effect of Barite Content on Anti Radiation Properties of Geopolymer Fly Ash Concrete Incorporated Natural Rock Ores of Hematite

Kahtan S. Mohammed<sup>1a</sup>, Ali Basheer Azeez<sup>2b</sup>, A. M. Mustafa Al Bakri<sup>3c</sup>, Kamarudin Hussin<sup>4d</sup>, Azmi B. Rahmat<sup>5e</sup>

<sup>1,2,3,4</sup>Center of Excellence Geopolymer & Green Technology (CEGeoGTech), School of Materials Engineering University Malaysia Perlis (UniMAP), 01000, P.O.Box, D/A Pejabat Pos Besar, Kangar, Perlis, Malaysia

<sup>5</sup>School of Materials Engineering, Universiti Malaysia Perlis (UniMap), Kompleks Pusat Pengajian Jejawi 2, 02600 Arau, Perlis, Malaysia

**Abstract:** *In this study, the effect of barite mineral (BaSO<sub>4</sub>) loading rates and its dispersive manner within two types of heavy constructive concrete matrix on anti radiation attenuation coefficients was investigated. To attain this goal geopolymer concrete based on fly ash and Ordinary Portland cement concrete of different barite additions were fabricated and examined. Similar proportions of natural mineral rocks (Hematite) rich in iron acquired from the north part of Iraq (Al-Sulaimanya site) as aggregates was added to the two concrete mixtures to enhance their density. Then fabricated cured and dried samples were assessed for their anti radiation attenuation properties. The attenuation measurements were performed using gamma spectrometer of NaI (TI) detector. The utilized radiation sources comprised <sup>137</sup>Cs and <sup>60</sup>Co radioactive elements with photon energies of 0.662 MeV for <sup>137</sup>Cs and average energy level about 1.25 MeV for the <sup>60</sup>Co. Likewise, the linear attenuation coefficient  $\mu$  (cm<sup>-1</sup>), mean free path mfp (cm), half value layer HVL(cm), Compressive Strength (Mpa), Density (kg/m<sup>3</sup>), Water Absorption (%) for the tested samples were obtained. The maximum linear attenuation coefficients ( $\mu$ ) were attained for ordinary concrete incorporates barite of 75 wt. %. They were of  $0.459 \pm 4.7 \times 10^{-2}$  for <sup>137</sup>Cs and  $0.371 \pm 3.3 \times 10^{-2}$  for <sup>60</sup>Co. For geopolymer they were of  $0.396 \pm 4.9 \times 10^{-2}$  for <sup>137</sup>Cs and  $0.316 \pm 4.7 \times 10^{-2}$  for <sup>60</sup>Co. Substantial improvement in attenuation performance by 15%–20% was achieved for concrete samples incorporate barite at different (15%–75%) loading rates. The microstructure, concrete density, homogeneity and particulate dispersion were examined using different metallographic, microscopic and measurement facilities. It was found that as the loading barite level is increased within the concrete mix the linear attenuation coefficient is improved for both the geopolymer and ordinary samples.*

**Keywords:** cement, barite, Geopolymer, concrete, NaI, Gamma-ray

## 1. Introduction

As neutron particles, X-ray and  $\gamma$ -ray are potentially harmful and can penetrate through the walls and roofs of generation and storage stations, therefore insulation is very important. These rays have high penetration power and can easily escape from accelerators and roofs of hospitals which house them [1].

Normal cement and building material don't have the ability to absorb and stop radioactive particles from escaping into the environment. Ordinary concrete is porous and tiny particles can easily pass through it. This is the reason that for insulation heavy concrete is used. Heavy concrete or insulation material consists of closely packed molecules which effectively prevent radioactive rays from penetrating through the walls and roofs. Insulation concrete is heavier and denser than normal cement. Medical units, radioactive plant, nuclear stations and generation plants use heavy concrete to make walls and roof radioactive proof [2, 3, and 4]. Also known as anti-radiation insulation concrete, heavy cement not only protects external environment from x-rays and radioactive particles but also used to absorb these rays. This is because radioactive particles have an ability to change direction after striking something and high density concrete significantly reduces the impact of these particles [2].

Anti-radiation concrete is almost 1.5 times heavier and denser than the ordinary cement and this is the reason that heavy concrete has better absorbing properties than normal cement. In order to formulate heavyweight concrete, one had to understand the importance of selecting appropriate ingredients. For example, ASTM C637-96 [5] and ASTM C638-92 [6] have the properties of increasing the density of concrete and make it a good radioactive absorbent.

Ordinary Portland Cement (OPC) is normally used in building roofs and walls but it is not as environment friendly as geopolymers, an insulation material used in the cement industry. However, fly-ash based geopolymers, a modified version of geopolymers, has improved adhesion properties and is denser than OPC. Geopolymers were used to limit the amount of energy required to manufacture OPC. Moreover, it has also reduced the emission of harmful gases, produced in manufacturing OPC to a significant extent [7-8]. According to an estimate, more than 13,500 million tons of harmful gases are emitted in the process of cement production, which account for almost 10% of the restricted gases produced annually [9-10].

There are some natural elements that have high density and good absorbing properties and Barite is one of them. With the chemical formula BaSO<sub>4</sub>, barite occurs in nature as the sulfate of Barium. When measured on Mohs scale of hardness, the hardness of crystalline Barite was found to be varying between 3 and 3.5. It means that the Barite matches

the scratch resistance of limestone. Moreover, this non-metallic crystalline material is 4-4.5 g/cm<sup>3</sup> dense [5]. However, one must be careful while using Barite for producing heavy concrete, as the crystal can be easily be crushed into powder and fine particles take longer to settle and harden[11]. Thickness of the insulation material depends on the amount of radiations to be absorbed and the energy levels of the radioactive particles [12].

A number of researchers like Akkurt et al., [13] opted for six mix designs to determine the attenuation coefficient of  $\gamma$ -ray. The study compared and examined a three mix design containing barite and another design containing limestone. Results of the study showed that the attenuation coefficient of  $\gamma$ -ray depends on the density of the concrete. Attenuation coefficient of  $\gamma$ -ray was found to be directly proportional to the density of the cement. Another important finding of the study indicated that varying the water to cementations ration did not have any influence on the attenuation coefficient of  $\gamma$ -ray.

Researcher S.J. Stankovic et al. [14] focused on the influence of aggregate material type on the radiation protection ability of heavy concrete. In order to compare the transmission factor, deposited energy and coefficients of mass attenuation of ordinary concrete and barite, photon transport Monte Carlo software program was used by the researcher. Results of the study proved that barite aggregates can considerably improves the radiation protection ability of cement. Moreover, it is far more effective in stopping and absorbing gamma rays than ordinary cement.

Akkurt et al. [15] I the study also investigated the effect of amount of barite or anti-radiation aggregates on the attenuation co-efficient of radioactive rays, findings of the study showed that attenuation coefficient is directly related to the type of material but there is no significant influence of quantity of aggregates on the radiation absorption ability of concrete.

The study of D. Mostofinejad et al. [1] focused on determining changes in the characteristics of heavy cement by varying factors like W/C ratio, quantity of pozzolanic

material and type of aggregates. The comparison was also used to evaluate the attenuation coefficient of heavy concentrate and ordinary cement (OPC). In order to measure the absorption of gamma rays, various experimental tests were conducted using advanced tools like XCOM software program. Findings of the study indicated that barite can increase the attenuation constant up to 30%. As far as the compressive strength is concerned, normal concrete showed higher level of compressive strength than heavy weight concrete at low W/C. However at higher W/C ratio, heavy concrete exhibits the same level of compressive strength as ordinary cement.

In the present study,  $\gamma$ -ray attenuation coefficients ( $\mu$ ) were determined for both heavy weight concretes with Portland cement and geopolymers content pozzolanic materials (FlyAsh) with constant amounts of hematite aggregates and different weight ratios of barite powder, incrementally increased from 15 to 70 wt. %.

## 2. Materials and Mixing Designs

### 2.1 The Raw Materials used to Prepare the samples of this work

In this study, the fly ash used was procured from Sultan Abdul Aziz power station in Kapar, Selangor, Malaysia, and equivalent to ASTM Class F with Specific Gravity ranges from 2.2 – 2.8. It was used as the base material to make the geopolymers. The compositions of the fly ash are given in Table 1. The composition analysis indicated that sum for SiO<sub>2</sub>, Al<sub>2</sub>O<sub>3</sub> and Fe<sub>2</sub>O<sub>3</sub> content was 81.72 wt. % which conforms to that of fly ash Class F type according to ASTM C-168 [16]. Fly ash geopolymer is based on fly ash and alkaline activator mixture of sodium silicate (waterglass) with 12M sodium hydroxide solution (NaOH). This molarity has been used by some previous researchers and shows higher compressive strength [17]. The normal scale and microstructure features of the original fly ash by SEM observation are shown in Figure.1 (a) and (b) respectively.

**Table 1:** XRF Analysis data of Fly Ash composition

Component	SiO <sub>2</sub>	Al <sub>2</sub> O <sub>3</sub>	Fe <sub>2</sub> O <sub>3</sub>	TiO <sub>2</sub>	CaO	MgO	SrO	K <sub>2</sub> O	SO <sub>3</sub>	Loss On Ignition(L.O.I)
Fly Ash%	51.2	16.3	13.67	1.20	11.1	2.2	0.243	1.34	2.25	4.4

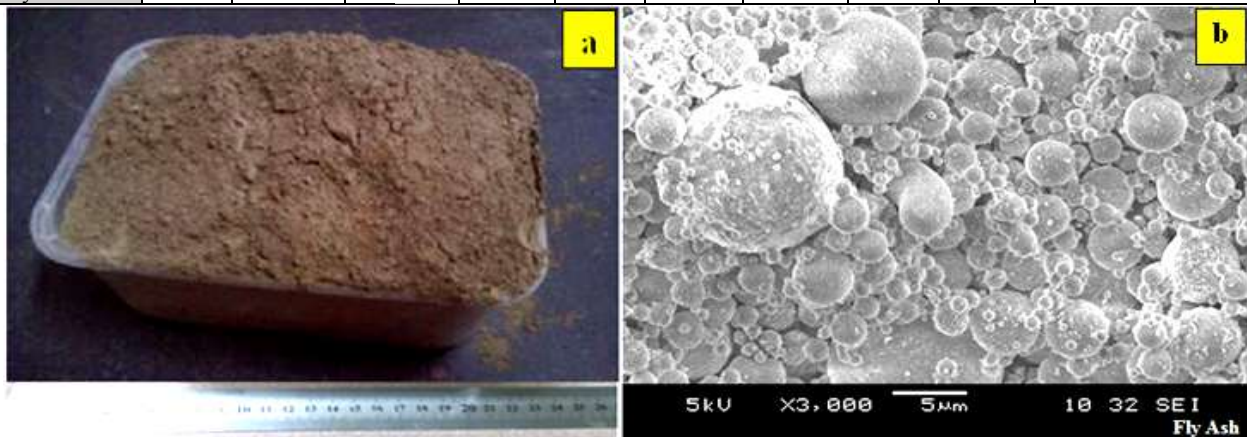


**Figure 1:** The fly Ash used in the geopolymers preparation in this study (a) normal scale optical graph (b) SEM micrograph reveals its microstructure features

The cement used in the present work was Ordinary Portland Cement (OPC) (Blue Lion brand) ASTM C150 Type 1. This type of cement is suitable for all purposes and widely used in construction projects, floors and other precast concrete panels. It complies with Malaysian standard (MS522) as well as the British Standard European Norm (BS EN

196).The specific gravity of Portland cement typically ranges from 3.10 to 3.25 with an average of 3.15. Table.2 shows the XRF analysis of OPC composition. The normal scale and SEM image for the powder features of OPC is shown in Figure.2 (a) and (b) respectively

**Table 2:** The XRF analysis of OPC composition

Component	SiO <sub>2</sub>	Al <sub>2</sub> O <sub>3</sub>	Fe <sub>2</sub> O <sub>3</sub>	P2O5	CaO	TiO <sub>2</sub>	SO <sub>3</sub>	K <sub>2</sub> O	Loss On Ignition(L.O.I)
OPC Type I	21.5	4.5	3.1	--	62.7	0.1	3.5	0.7	1.3

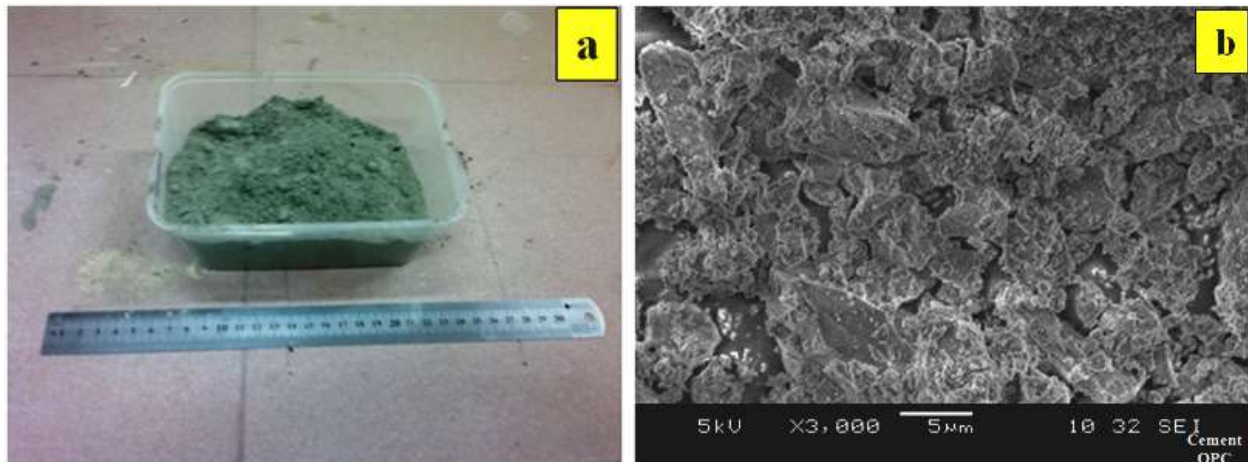


**Figure 2:** The OPC used in this work (a) normal scale optical graph (b) SEM image exhibits its microstructure.

The aggregates used to prepare the tested samples in this study were natural ore rocks (Hematite rich in iron) from the north part of Iraq (Al Sulaimanya governorate). Table.3 shows the XRF analysis of these aggregates. Figure 3(a) and (b) shows the hematite rocks before and after crushing

respectively. Figure .4(a) and (b) shows the SEM and the energy dispersive spectroscopy (EDS) analysis for these aggregates.

**Table 3:** XRF analysis of the aggregate composition

Component	SiO <sub>2</sub>	Al <sub>2</sub> O <sub>3</sub>	Fe <sub>2</sub> O <sub>3</sub>	CaO	MgO	SO <sub>3</sub>	MnO	Loss on ignition (L.O.I)
hematite Aggregate %	14.65	3.93	50.79	9.74	4.55	0.03	2.45	12.45



**Figure 3:** Optical graphs (a) show the hematite rocks before crushing (b) after being crushed to suitable sizes.



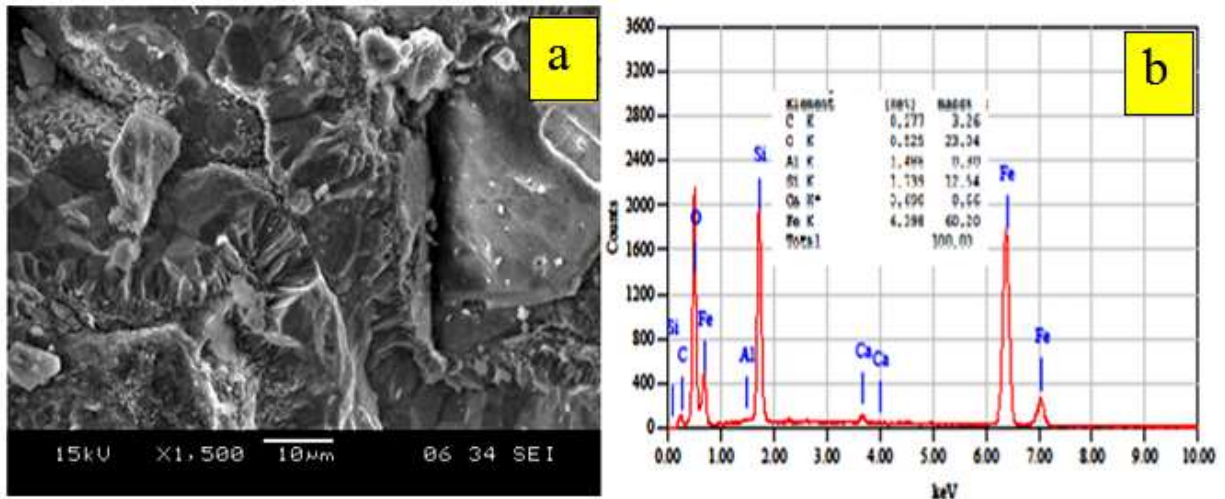


Figure 4: (a) SEM image reveals the microstructure of the Hematite rock aggregates and (b) the EDS analysis.

Barite is a mineral composed of barium sulfate ( $BaSO_4$ ). This name is in response to the high specific gravity of barite which is of  $4.5 \text{ g/cm}^3$  and it is exceptional for a nonmetallic mineral. This makes barite suitable for a wide ranges of applications; it has many advantages, such as good stability, strong chemical inert, acid and alkali proof, moderate rigidity, high density, high whiteness, high specific gravity, harmful rays absorbing ( $\gamma$ -ray & X-ray), it is widely used in the fields of paint, chemistry, rubber, glass, pottery, and paper. Barite also serves as the principal ore of barium. In this study, the barite used was acquired from China zhashui heqi barite mining Co.ltd. Table 4 shows the

XRF chemical analysis of barite. The used in this study and the photography microstructure of the original barite on the SEM observation are shown in The optical and SEM images of barite powder in Figure.5 (a) and (b) shows the as received barite powder and its microstructure respectively.

Table 4: The XRF analysis data of barite composition

Component	BaSO <sub>4</sub>	SrSO <sub>4</sub>	SiO <sub>2</sub>	CaCO <sub>2</sub>	Fe <sub>2</sub> O <sub>3</sub>
Barite %	90.8	0.1	8.4	0.3	0.5

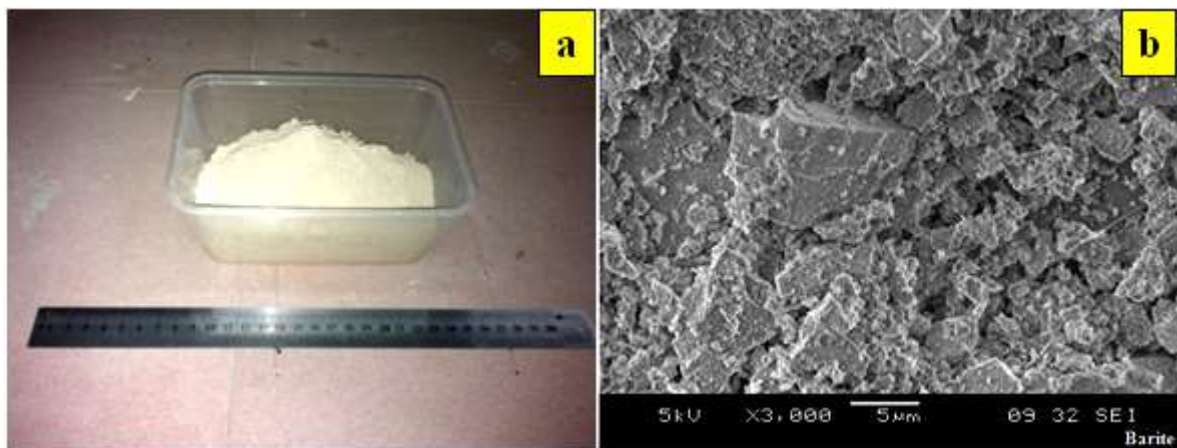


Figure 5: (a) As received barite powder (b) SEM image of the barite microstructure

### 2.2 Mixing Designs

The ore rocks were crushed and sieved to separate the fine aggregates from the coarse ones. The sieve size analysis for the ore fine aggregates (sand) used in this study is exhibited in Table 5.

Table 5: the size sieve analysis for the fine aggregates used in this study.

Sieve(mm)	Passing (%) sand	Passing (%) Aggregates
9.5	--	100
6.5	--	60
4.75	100	25
2.38	98.75	0
1.19	95	--

0.59	70	--
0.30	40	--
0.15	10	--

Two sets four samples each of Portland cement and fly ash geopolymer heavy weight concrete mixtures containing similar hematite aggregates ratios and different barite ratios incrementally increased from 15 to 70 wt. % were prepared. Figure 6 (a) and (b) shows these tested samples.

The high density geopolymer concrete compositions and heavy ordinary concrete prepared from the hematite aggregates and different weight ratios of barite were used to prepare block samples for gamma and X-ray shielding

according to the American code standard (ASTM C638; ASTM C637) [5,6].

For the composition of geopolymer concrete samples, the ratios of solid/liquid (S/L) and sodium silicate/ NaOH used were constant for all samples mixtures. The alkaline activator/fly ash ratio was 2.5. The alkaline activator was a mixture of sodium waterglass ( $\text{Na}_2\text{SiO}_3$ ) and sodium hydroxide (NaOH) solution was prepared and mixed at constant  $\text{Na}_2\text{SiO}_3/\text{NaOH}$  solution ratio of 2.5 [18]. For the concrete mixture of Ordinary black Portland cement, the tested samples were produced according to ASTM C637.

Reference concrete mixes ratio 1:2:4 consisted of cement  $1\text{kg/m}^3$ , sand  $2\text{kg/m}^3$ , gravel  $4\text{kg/m}^3$ , and water  $0.4\text{kg/m}^3$  were adopted. The water to cement (w/c) ratio was 0.4.

The microstructure and the macrostructure of the two types of the concrete tested samples have been investigated. Figure 7 shows low magnification optical fractograph of (a) ordinary concrete sample and (b) geopolymer concrete sample. Both samples have 75 wt. % of barite. The fractographs reveal the distribution of barite and hematite aggregates within the concrete matrix.

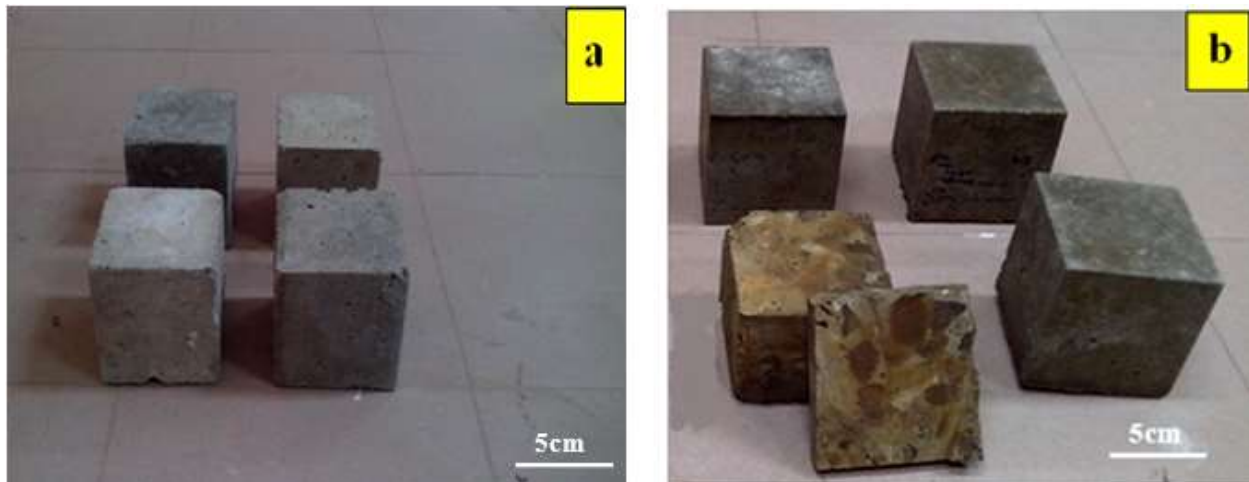


Figure 6: The molded samples used in this study (a) the ordinary concrete sample (b) the geopolymer concrete samples.

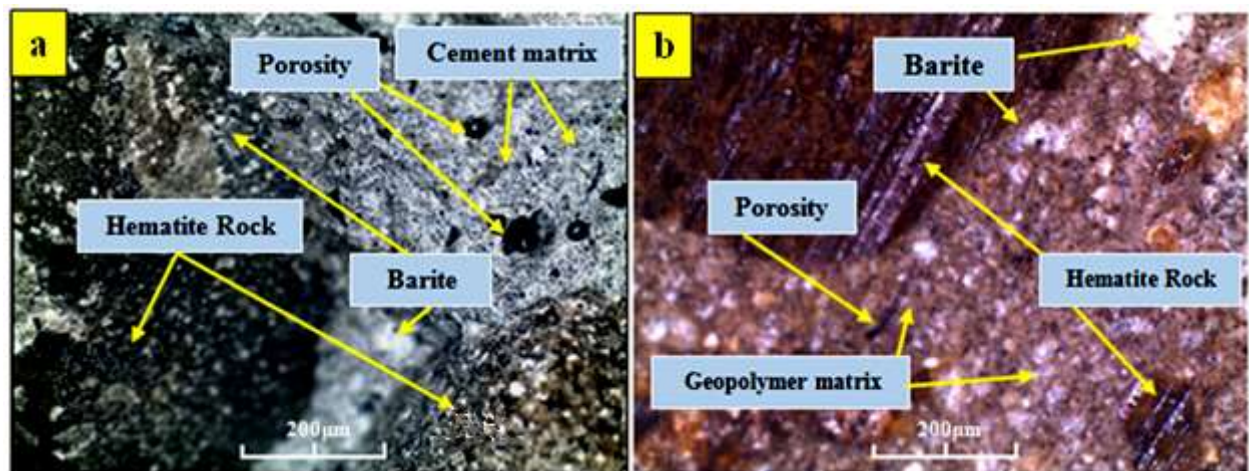


Figure 7: shows low magnification optical fractograph of (a) ordinary concrete sample and (b) geopolymer concrete sample.

### 3. Experimental and Testing

#### 3.1. Molding, Curing and Compressive Strength Test

After 10 min of mechanical mixing, the fresh homogeneous geopolymer mixture was placed in (100 x 100 x 100) mm standard steel molds. The samples were compacted with two layer placing as described in ASTM C109. Then they were cured at  $70\text{ }^\circ\text{C}$  for 24 hr by putting them in low temperature electrical furnace (L T Furnace, L6-1200). Water evaporation was prevented by sealing the top of the molds with a thin plastic layer during storage as well as during the curing stage. After curing time elapsed, the molds were taken out of the furnace and left to cool down to room

temperature before demolding and left to be cured for 28 days at room temperature. For Portland cement samples, the same procedure was followed except that the initial 24h curing time was conducted at room temperature. After that the samples were cured by immersing them in water for 28 days. The compressive strength test was conducted on three cured hardened samples of the geopolymer and the ordinary concrete types using Shimadzu Universal Testing Machine and the average strength was calculated.

#### 3.2. Density and Water Absorption Calculation

The water absorption was determined according to ASTM C642 and equation. 1, the size of the sample for water absorption tests was (100 x 100 x 100) mm. The test was



done by immersing the samples in the water for 24 h and the difference in weight before and after immersion was measured. The amount of water absorbed for each sample was determined by measuring the weight difference using 0.1 mg accuracy electronic balance.

$$\text{Water absorption} = [(M_s - M_d) / M_d] \times 100 \quad (1)$$

Where,  $M_s$  is the mass of surface-dried sample (g) and  $M_d$  is the mass of oven-dried sample (g).

The porosity was determined according to ASTM C642 and was calculated by the equation 2:

$$\text{Porosity} = [(M_w - M_d) / (M_w - M_s)] \times 100 \quad (2)$$

Where,  $M_w$  is the mass of specimen after immersion in water (g),  $M_d$  is the mass of specimen after oven dried (g) and  $M_s$  is the mass of specimen suspended in water (g).

Density of samples was calculated according to equation 3.

$$\text{Density (Kg/m}^3) = \frac{\text{Mass of sample (Kg)}}{\text{Volume of samples (m}^3)} \quad (3)$$

### 3.3 Measurements of Gamma $\gamma$ -ray Attenuation Coefficient

The experimental work for radiation test consists of two steps. In the first step, the attenuation was examined by measuring the ratio of the penetrating radiation through the three axes of each cube. The average values and the standard deviations for the readings were calculated to acquire the accuracy of the measurements and to assure the homogeneity of the cubes in each sample. In the second step the cubes were cut into slabs with different thicknesses to establish the attenuation plots and consequently to calculate the half value layer (HVL) for each sample.

The attenuation measurements were performed using gamma ray spectrometer of 3"  $\times$  3" NaI (Tl) detector with a Multi Channel Analyzer (MCA). The spectrometer communicates with the personnel computer (PC) by Genie200 software. The emitting photon energies of the utilized  $^{137}\text{Cs}$  and  $^{60}\text{Co}$  sources were of 0.662, 1.25 MeV respectively. The linear attenuation coefficients for these samples were experimentally determined using narrow collimated monoenergetic beam of gamma rays. The schematic representation of the experimental setup is shown in Figure 8.

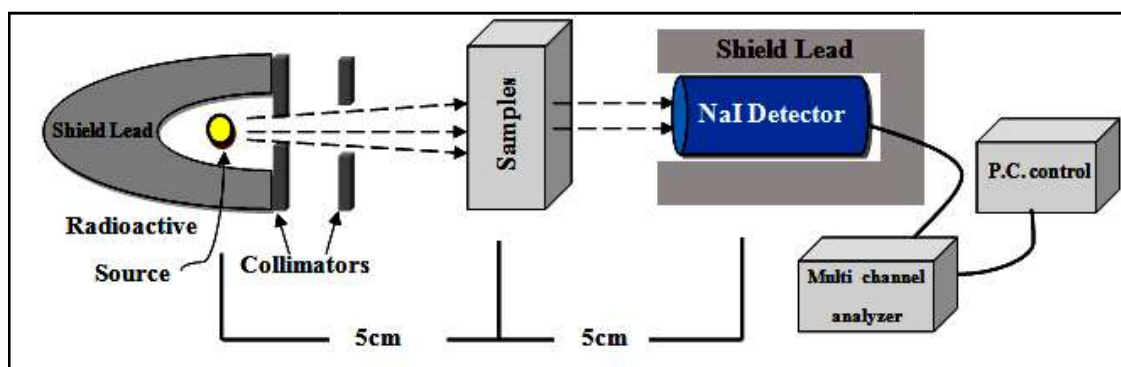


Figure 8: Schematic representation of the setup of the measurements.

Background was subtracted from the initial intensity ( $I_0$ ) and the Intensity ( $I$ ) of the transmitted beam. The density ( $\rho$ ) is mass and volume dependant. The linear attenuation coefficients  $\mu$  was determined by measuring the transmission of gamma-rays through a target i.e. sample of known thickness. The area under the curve of the photo peak spectrum is used to evaluate the intensity  $I$  of the transmitted beam. Evaluation of  $I_0$  which is the area under the photo peak is obtained without inserting any sample between the detector and the source, from  $I$  and the incident photon  $I_0$  for thickness  $x$  which is the distance between the detector and the source, the linear attenuation coefficients  $\mu$  is given by the following formula:

$$\mu = \frac{1}{x} \ln \frac{I_0}{I} \quad (4)$$

The mean free path  $mfp$  is the average distance the photon travels between collisions with the atoms of the target material. It can be taken as the length of the path divided by the number of collisions. The  $mfp$  depends on the material characteristics and the energy of the radiated photons [19]. It is related to the attenuation by the following formula:

$$mfp = \mu^{-1} \quad (5)$$

The following formula is used to calculate the values of the standard deviations at 8 positions of each implemented sample:

$$\sigma(\bar{\mu}) = \frac{\sqrt{\sum (\mu_i - \bar{\mu})^2}}{N - 1} \quad (6)$$

Where,

$\sigma(\bar{\mu})$  : is the standard deviation at any position.

$\mu_i$ : is the linear attenuation coefficient at any position of the Sample.

$\bar{\mu}$  : is the average value of the linear attenuation coefficient.

$N$ : is the number of the measured positions for each sample, in this study they were 8 positions.

### 4. Results and Discussion

The average values of the linear attenuation coefficient and their standard deviations, the half value level, the mean free path, then compressive strength, density and water absorption for the four sets of both concrete samples at two gamma-ray energies are given in Table.6. Their radioactive sources were of 0.662MeV and about 1.25MeV for  $^{137}\text{Cs}$  and  $^{60}\text{Co}$ , respectively.

It is clear from Table.6 that the values of the standard deviations are small and varied from 0.01 to 0.05. This gives good indication that the fabricated samples have good homogeneity and of even distributions of the dense components within the concrete cohesive mixture. The value for the fabricated samples was increased specially for

samples no (4) which contains higher mixing wt. % ratio of barite. In fact, sample 4 produced attenuation which is better than other samples by about 11% at 0.662 MeV for <sup>137</sup>Cs radioactive source.

**Table 6:** The average values of linear attenuation coefficient with standard deviation, the half value level, mean free path, the compressive strength, density and water absorption for the both geopolymer and ordinary concrete were tested

Type of samples	Radioactive source	Samples	Samples 1	Samples 2	Samples 3	Samples 4	
		Barite to sand wt. %.	15%	30%	50%	75%	
		Parameters					
Geopolymer concrete	<sup>137</sup> Cs 0.663 MeV	$\bar{\mu}$ (cm <sup>-1</sup> ) and $\sigma(\bar{\mu})$	0.317±0.010	0.351±0.015	0.382±0.021	0.396±0.049	
		HVL (cm)	2.18	1.97	1.81	1.75	
		Mfp (cm)	3.15	2.84	2.61	2.52	
	<sup>60</sup> Co 1.25 MeV	$\bar{\mu}$ (cm <sup>-1</sup> ) and $\sigma(\bar{\mu})$	0.177±0.012	0.183±0.035	0.214±0.018	0.316±0.027	
		HVL (cm)	3.91	3.78	3.23	2.00	
		Mfp (cm)	5.64	5.46	4.67	2.89	
			Compressive Strength (Mpa)	76.67	87.11	70.75	59.25
			Density (kg/m <sup>3</sup> )	2894	3186	3398	4189
			Water Absorption (%)	4.59	4.01	3.58	3.97
Ordinary concrete	<sup>137</sup> Cs 0.663 MeV	$\bar{\mu}$ (cm <sup>-1</sup> ) and $\sigma(\bar{\mu})$	0.311±0.014	0.382±0.018	0.412±0.014	0.459±0.047	
		HVL (cm)	2.22	1.81	1.68	1.51	
		Mfp (cm)	3.21	2.61	2.42	2.17	
	<sup>60</sup> Co 1.25 MeV	$\bar{\mu}$ (cm <sup>-1</sup> ) and $\sigma(\bar{\mu})$	0.187±0.052	0.193±0.036	0.243±0.011	0.371±0.033	
		HVL (cm)	3.70	3.59	2.85	1.86	
		Mfp (cm)	5.34	5.18	4.11	2.69	
			Compressive Strength (Mpa)	31.11	32.68	15.53	16.33
			Density (kg/m <sup>3</sup> )	2945	3283	3530	4438
			Water Absorption (wt. %)	4.97	5.02	4.72	4.38

The linear attenuation coefficients  $\mu$  for both concretes types containing different wt. % of barite was measured. The results for two radiation sources of <sup>137</sup>Cs of 0.662 MeV energy and <sup>60</sup>Co of MeV1.25 energy are displayed in Figures 9 and 10. It is very obvious from the two plots that the linear

attenuation coefficients for geopolymer and ordinary concrete were increased with increasing the wt. % of barite content in the tested samples

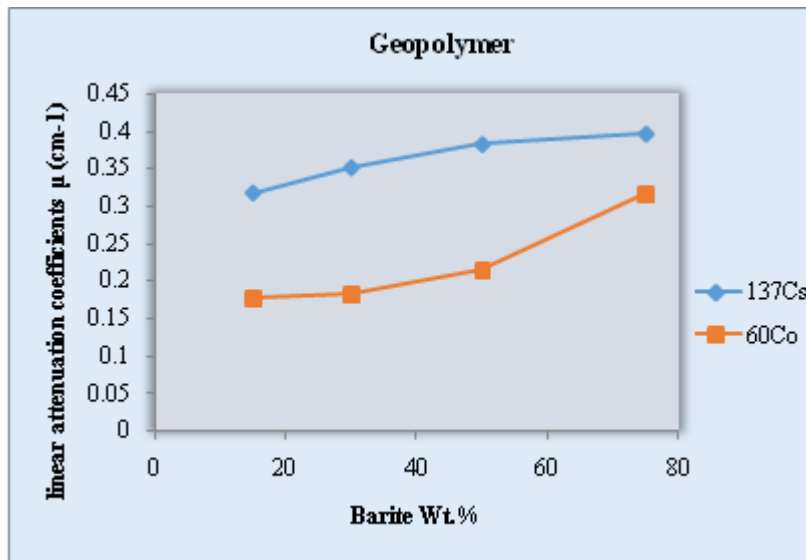


Figure.9: The linear attenuation coefficients for geopolymer samples at energies for  $^{137}\text{Cs}$  and  $^{60}\text{Co}$  sources with wt. % of barite

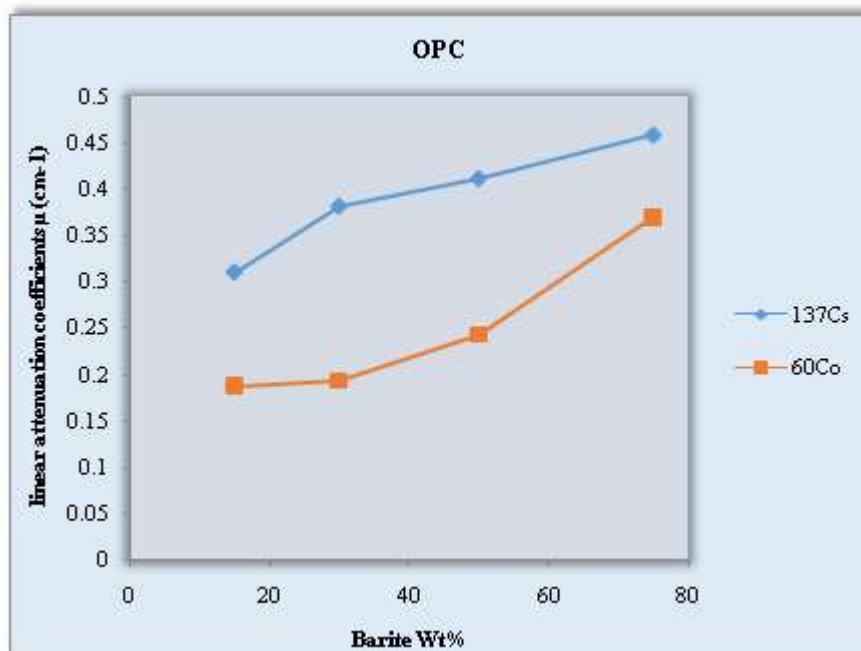


Figure 10: The linear attenuation coefficients for ordinary concrete samples at energies for  $^{137}\text{Cs}$  and  $^{60}\text{Co}$  sources with wt. % of barite

The concrete samples incorporated natural rocks aggregates rich in hematite and of 75 wt. % barite showed the highest linear attenuation coefficients as opposed to the other tested samples of both types. This is attributed to the high specific gravity of barite and hematite aggregates within the concrete mixture which led to high overall density of the concrete mixture. This mixture showed reduction in pores that additionally enhances the concrete density. The plot in Figure 11 shows the variation of samples density vs. barite wt. % for geopolymer and ordinary concrete tested samples. It can be seen that samples density increased as the wt. % of barite increased. The correlation between the samples' density and barite wt. % is used to confirm the linearity; it is obvious that barite is effective in diminishing the transmission of radiation. The samples used OPC has slightly larger value of density as compared to the samples of geopolymer. This is due to the higher specific gravity of

ordinary OPC which ranges from 3.10 to 3.25 as compared to 2.2 to 2.8 specific gravity of fly ash geopolymer.

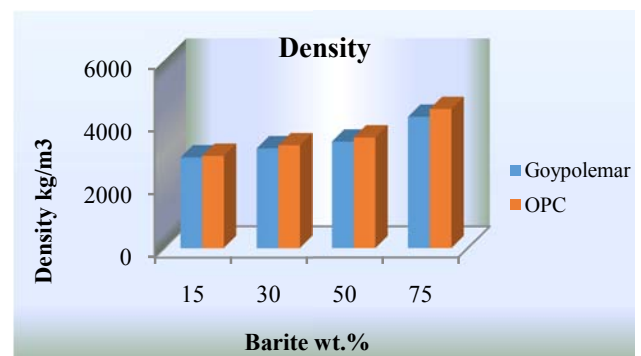
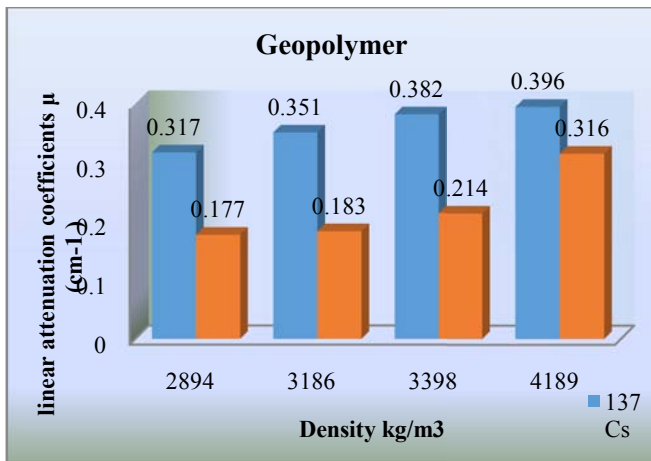


Figure 11: The sample's density as a function of the barite wt. % contended of the both geopolymer and ordinary samples.



Back to Table.6, the HVLs are inversely proportional to the average linear attenuation coefficient values. This is indicated clearly by the result demonstrates the relation between  $\bar{\mu}$  and the HVL. It is obvious that when the shielding material has large absorption potential of the incident radiation the recommended thickness of the shield will be substantially reduced. It is also apparent from the results that the mfp decreased when the linear attenuation coefficients increased. This came in accord with the definition of the mean free path, wherein the probability of many successive collisions means small mean free path and consequently large attenuation.

As the radiation shielding capability depends on material's density, it is important to plot the linear attenuation coefficients against samples density. These plots are displayed in Figure 12 and Figure 13 for both geopolymer and OPC samples respectively; it is clearly shown that the linear attenuation coefficients increased with increasing samples density.



**Figure 12:** The measured linear attenuation coefficient of geopolymer concrete sample against samples density at  $^{137}\text{Cs}$  and  $^{60}\text{Co}$  energy levels.

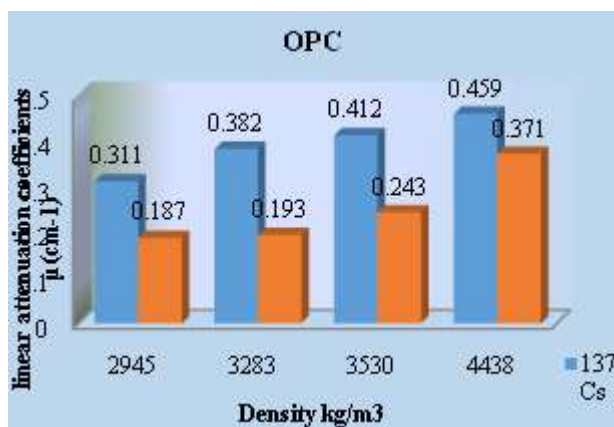


**Figure 13:** The measured linear attenuation coefficient for OPC sample against sample density at  $^{137}\text{Cs}$  and  $^{60}\text{Co}$  energy levels.

The compressive strength was acquired for three 28 days cured hardened geopolymer and OPC samples at room temperature and in water respectively. The average strength was calculated for different samples, the values of compressive strength are displayed in Figure 14. It can be

seen from this figure that the compressive strength decreased when the barite wt. % is increased in the molded samples. This reveals that barite deteriorates the concrete strength. The plot in Fig 14 shows a comparison between the compressive strength of geopolymer and OPC samples. The compressive strength of samples comprised fly ash geopolymer is much better than that contained OPC. This is attributed to the much stronger chemical bond between geopolymer components such as  $\text{SiO}_2$  and  $\text{Al}_2\text{O}_3$  than the chemical interaction in concrete contains OPC as evident in XRD analysis.

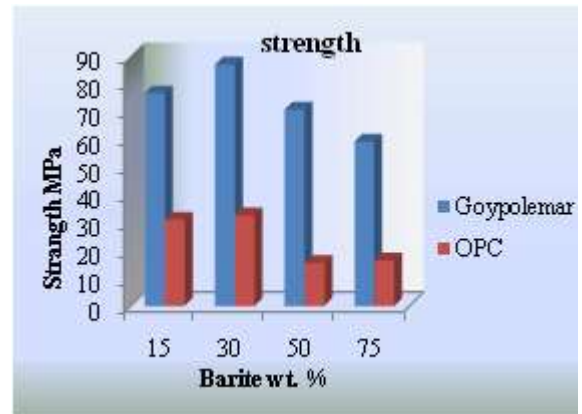


**Figure 14:** The compressive strength for geopolymer and OPC contains different barites wt. %

## 5. Conclusions

During this study, strict screening, sizing, cleaning and classification procedure for barite addition were implemented.

1. The maximum linear attenuation coefficients ( $\mu$ ) were attained for ordinary concrete incorporates barite of 75 wt. %. They were of  $(0.459 \pm 4.7 \times 10^{-2})$  for  $^{137}\text{Cs}$  and  $(0.371 \pm 3.3 \times 10^{-2})$  for  $^{60}\text{Co}$  and for geopolymer they were  $(0.396 \pm 4.9 \times 10^{-2})$  for  $^{137}\text{Cs}$  and  $(0.316 \pm 4.7 \times 10^{-2})$  for  $^{60}\text{Co}$ .
2. Samples incorporated OPC has slightly better results than geopolymer samples because of the relatively superior specific gravity of OPC Compared with fly ash. This justifies the higher density of OPC samples than that of geopolymer samples.
3. The results proved that addition of powder barite have great impact on attenuation performance of the concrete samples besides its positive impact on the bulk density and porosity level of the solidified concrete mixtures for both types.
4. However, it is found that compressive strength decreased as the barite contents augment in the concrete mixtures for both types of concrete samples.
5. It was obvious that compressive strength of geopolymer used fly ash and incorporated similar amounts of hematite natural ores and barite is much better than its counterpart of OPC. this is because of the chemical bond by in a reaction components geopolymer stronger than from chemical bond in the interaction of ordinary concrete, owing the Contents of the  $\text{SiO}_2$  and  $\text{Al}_2\text{O}_3$  on fly ash larger than in OPC as evident in XRD analysis.
6. These finding indicates that there is a good potential to use barite as fine aggregates, cementitious material and

density promoter within anti radiation heavy concrete mixtures.

## References

- [1] D. Mostofinejad, M. Reisi and A. Shirani; Mix design effective parameters on c-ray attenuation coefficient and strength of normal and heavyweight concrete; *Construction and Building Materials*; 28 (2012) 224–229.
- [2] ACI Committee 304. Guide for measuring, mixing, transporting, and placing concrete, ACI 304R-00. American Concrete Institute; 2009. 41 pp.
- [3] ACI Committee 116. Cement and concrete terminology, ACI 116R-00. American Concrete Institute; 2009. 73 pp.
- [4] Topcu IB. Properties of heavyweight concrete produced with barite. *Cem Concr Res* 2003; 33:815–22.
- [5] ASTM C637-96. Standard specification for aggregates for radiation-shielding concrete, vol. 04.02. Annual Book of ASTM Standard; 1997. p. 297–9.
- [6] ASTM C638-92. Standard descriptive nomenclature of constituents of aggregates for radiation-shielding concrete, vol. 04.02. Annual Book of ASTM Standard; 1997. p. 300–2.
- [7] Chindaprasirt P., Chareerat T., and Sirivivatnanon V., —Workability and Strength of Coarse High Calcium Fly Ash Geopolymer. *Cement and Concrete Composites*, Vol. 29, pp. 224-229, (2007).
- [8] Malhotra V.M., —Introduction: Sustainable Development and Concrete Technology. *ACI Concrete International*, Vol. 24 (7), (2002).
- [9] A.M. Mustafa Al Bakri, H. Kamarudin, M. BinHussain, I. Khairul Nizar, Y. Zarina & A.R. Rafiza; The Effect of Curing Temperature on Physical and Chemical Properties of Geopolymers; 2011 International Conference on Physics and Science and Technology (ICPST 2011); [www.elsevier.com/locate/procedia](http://www.elsevier.com/locate/procedia).
- [10] Van Jaarsveld J.G.S., van Deventer J.S.J., and Lukey G.C., —The effect of Composition and Temperature on the Properties of Fly Ash and Kaolinite-based Geopolymers. *Chemical Engineering Journal*, Vol. 89, pp. 63-73, (2002).
- [11] Neville AM. *Properties of concrete*. 4th ed. Wiley; 1996.
- [12] I. Akkurt, H. Akyildirim, B. Mavi, S. Kılınçarslan, and C. Basyigit, The Effect of Pumice Rate on the Gamma Absorption Parameters of Concrete; *Proceedings of the International Congress on Advances in Applied Physics and Materials Science, ACTA PHYSICA POLONICA* Vol. 121; 144-146, (2012).
- [13] Akkurt I, Basyigit C, Skilincarsan S, Mavi B. The shielding of c-rays by concretes produced with barite. *Progress Nucl Energy*; 46:1–11; 2003.
- [14] S.J. Stankovic, R.D. Ilic, K. Jankovic, D. Bojovic, and B. Loncar; Gamma Radiation Absorption Characteristics of Concrete with Components of Different Type Materials; *Selected papers presented at the Eleventh Annual Conference of the Materials Research Society of Serbia, YUCOMAT 2009*, Vol. 117; 812-816: (2010)
- [15] Akkurt I, Basyigit C, Skilincarsan S, Mavi B, Akkurt A. Radiation shielding of concrete containing different aggregates. *Cem Concr Compos*; 28:153–7. 2006.
- [16] Chindaprasirt P, Chareerat T, Sirivivatnanon V. Workability and strength of coarse high calcium fly ash geopolymer. *Cem Concr Compos* 2007; 29:224–9.
- [17] Ubolluk Rattanasak, Prinya Chindaprasirt, “Influence of NaOH solution on the synthesis of fly ash geopolymer,” *Mineral Engineerings*, vol. 22, pp. 1073-1078, 2009.
- [18] Palomo A, Grutzeck MW, Blanco MT., “Alkali-Activated Fly Ashes, A Cement for the Future,” *Cement & Concrete Research*, vol.29, pp. 1323-9, 1999.
- [19] Ali, B.A.; Kahtan, S.M.; Andrei, V.A.; Abdullah, M.M.; Hussin, K.; Ioan, G.S. Evaluation of Radiation Shielding Properties for Concrete with Different Aggregate Granule Sizes. *Rev. Chim.* 2013, 64, 899–903.